Short Communication

Analysis of the performance of $In_xGa_{1-x}N$ based solar cells

Carlos A. Hernández-Gutiérrez[1] · Arturo Morales-Acevedo[2] · Dagoberto Cardona[3] · Gerardo Contreras-Puente[4] · Máximo López-López[5]

Abstract

We have modeled $In_xGa_{1-x}N$ single homo-junction solar cells considering realistic carrier transport parameters. It is shown that the maximum efficiency will be less than 19% for an Indium content around 60%. This practical efficiency limit is due to technological issues such as the residual high electron background making it difficult to have p-type doping, causing a low open circuit-voltage and the reduction of the absorber depletion region, and as a result a drop in the photo-current generation. Besides, the difficulty for incorporating In concentrations higher than 40% without phase separation in addition to highly defective material should also be considered. The model does not take in account the carrier lifetime variation as a function of the In content because there are no experimental studies about this yet. To overcome this lack of knowledge, the solar cell with the highest possible In content was modeled by varying the carrier lifetimes from picoseconds to nanoseconds giving calculated efficiencies in the range from 3.9 to 18.9%, respectively. These results explain the poor experimental efficiencies already reported for $In_xGa_{1-x}N$ single homo-junction solar cells and suggest that, even in the best case, the expected efficiency will be below that obtained for more conventional Si and GaAs solar cells. Hence, our analysis indicates that alternative ways, such as using nanoparticles or nanowires engineered for making competitive solar cells using this kind of materials, should be looked for in the near future.

Keywords InGaN · Solar cells · Efficiency · Carrier lifetime · Defects

1 Introduction

The $In_xGa_{1-x}N$ has been considered a material with great potential to achieve high efficiency in tandem solar cells because the energy gap (Eg) can be varied from 0.7 to 3.4 eV [1]. However, even after nearly 20 years of research and significant incremental contributions, only a few reports have shown a small efficiency improvement [2–4]. Some reasons for this are the following technological challenges:

The first and the most important challenge is the difficulty to incorporate the adequate Indium concentration at the absorber layer. Typically, when Indium concentration exceeds 20%, the obtained ternary alloy tends to show phase separation and this problem gets worse as the thickness of the $In_xGa_{1-x}N$ layer increases [5–7]. Fischer et al. [8] have estimated the critical thickness of the stressed $In_xGa_{1-x}N$ before phase separation appears, obtaining a thickness of 12 nm for Indium concentrations around 25%, and as the concentration increases the critical thickness is reduced. Although $In_xGa_{1-x}N$ has a high absorption coefficient, films with an adequate thickness are difficult to achieve without the phase separation occurring. So, as the concentration of In increases in the ternary, the crystalline quality is reduced [9, 10].

The second challenge is the difficulty to control the p-type conductivity due to the high background electron concentration in $In_xGa_{1-x}N$. Moreover, Mg doping has

✉ Arturo Morales-Acevedo, amorales@solar.cinvestav.mx | [1]Nanoscience and Nanotechnology Doctoral Program, CINVESTAV-IPN, 07360 Mexico City, Mexico. [2]Electrical Engineering Department SEES, CINVESTAV-IPN, 07360 Mexico City, Mexico. [3]Mathematics and Physics Department, ITESO, 45604 Tlaquepaque, Jalisco, Mexico. [4]ESFM, Instituto Politécnico Nacional, 07738 Mexico City, Mexico. [5]Physics Department, CINVESTAV-IPN, 07360 Mexico City, Mexico.

SN Applied Sciences (2019) 1:628 | https://doi.org/10.1007/s42452-019-0650-x

Received: 26 February 2019 / Accepted: 19 May 2019 / Published online: 24 May 2019

shown low dopant activation efficiencies around 1% for GaN. As a result, high Mg concentrations near the atomic solubility should be introduced into the films. Thus, under certain synthesis conditions the Mg tends to generate donors that compensate the p-type conductivity [11]. The difficulties for obtaining p-type $In_xGa_{1-x}N$ with relatively high In-content have been attributed to the high background electron concentrations caused by the low $In_xGa_{1-x}N$ growth temperature which seems to promote the incorporation of donor like defects and impurities [12]. Finally, the third technological challenge is the difficulty to fabricate Ohmic contacts with a low specific contact resistance due to the large work functions ~ 6 eV for p-GaN [13].

For overcoming these technological issues, several approaches have been attempted such as the fabrication of (pin) double hetero-structures p-GaN/$In_xGa_{1-x}N$/n-GaN and solar cells based on $In_xGa_{1-x}N$/GaN multi-quantum wells (MQWs), but poor efficiencies of less than 3.5% have been reported [14–16]. In addition, another important aspect worth mentioning is that the use of double hetero-structures such as GaN/$In_xGa_{1-x}N$/GaN will cause the appearance of a potential barrier at each interface, increasing the solar cell series resistance. The main contribution of this work is to establish a practical upper limit efficiency that can be obtained with solar cells based on $In_xGa_{1-x}N$, considering the opto-electronic properties of these materials and the technological difficulties to obtain good material properties and device structures for achieving high efficiencies. These technological difficulties have not been overcome for 20 years and the arguments presented here suggest that they may not be overcome. Therefore, if the maximum expected efficiency for homojunction $In_xGa_{1-x}N$ based solar cells does not exceed the efficiencies of more conventional solar cells such as Si or GaAs, then a new approach is needed. For example, using $In_xGa_{1-x}N$ nanoparticles for making quantum dot solar cells or implementing a graded band-gap absorber layer (varying x gradually) as has been suggested for CdZnTe [17].

2 Solar cell structure

In this work, a homo-junction solar cell structure was chosen, according to the technological difficulties and the experimental advances already reported in the literature, as the most appropriate to be experimentally fabricated. This structure has been experimentally done by Valdueza-Felip et al. [14], with a high In content at the absorber layer (40%) and large hole concentration in the p-type layer. The structure starts with a substrate such as Sapphire, SiC or Si(111) in order to provide an epitaxial seed for III-Nitrides hexagonal phase. Sapphire is chosen because GaN grows on it with a low dislocation density at a low cost in comparison with SiC substrates. Subsequently, an AlN buffer layer is deposited followed by a second GaN buffer layer to reduce the dislocation density to the minimum possible. Then, a n-type $In_xGa_{1-x}N$:Si layer with a very high electron concentration (10^{19} cm^{-3}) which acts as a back surface field (BSF) should be added. After that, a non-intentionally doped (nid) $In_xGa_{1-x}N$ absorber layer should be synthesized. We refer to this (nid) layer because the residual electron concentration is high, and its compensation is a current technological challenge. Finally, the p-type $In_xGa_{1-x}N$ emitter layer should be synthesized. According to [14], an $In_xGa_{1-x}N$ p-type layer with a hole concentration of 3×10^{18} cm^{-3} can be achieved. Therefore, the maximum hole concentration that we can consider in this model is 3×10^{18} cm^{-3} due to the difficulty to obtain higher hole concentrations. In addition, it is important to mention that the p-type layer should be deposited as the top layer because Mg doping degrades the crystalline quality of the material, which in turn may increase its roughness [12, 14, 15]. In other words, if the structure were synthesized over the p-type layer, poor crystalline quality and roughness are expected to spread throughout the structure reducing the crystalline, optical and electrical properties. Moreover, it is worth mentioning that the p-$In_xGa_{1-x}N$ layer doping concentration is a key parameter to achieve an adequate depletion layer width. Assuming a free hole concentration of 10^{18} cm^{-3} in the p-$In_xGa_{1-x}N$ layer and according with Ref. [2], it is reasonable to consider that the residual electron concentration in the $In_xGa_{1-x}N$ absorber layer should also be ~ 10^{18} cm^{-3}. Then, if the hole concentration is less than 10^{18} cm^{-3}, the depletion region will extend mainly over the emitter layer instead of the base layer, reducing the photo-collection within the (base) depletion region and in turn reducing the efficiency. In addition, if the hole concentration in the p-layer is less than 10^{18} cm^{-3}, a Schottky barrier at the top contact might be achieved instead of the desired Ohmic contact. So, the hole concentration must be at least 10^{18} cm^{-3} to have a reasonable photocurrent generation (in the depletion region) and to avoid the possible formation of a Schottky barrier at the metal contact. The proposed structure is illustrated in Fig. 1. Therefore, considering the present technological issues, the homojunction structure is chosen because it should present low dislocation density, low surface roughness, no barrier potentials at the interfaces as in the case of double heterostructure solar cell (GaN/$In_xGa_{1-x}N$/GaN), an adequate depletion region width, and simple Ohmic contact formation at top of the p-$In_xGa_{1-x}N$ emitter layer.

3 Modeling

An analytical model was employed to calculate the efficiency that can be achieved with homo-junction $In_xGa_{1-x}N$ solar cells. The model includes the In content effect on the photocurrent and the effect of high residual electron

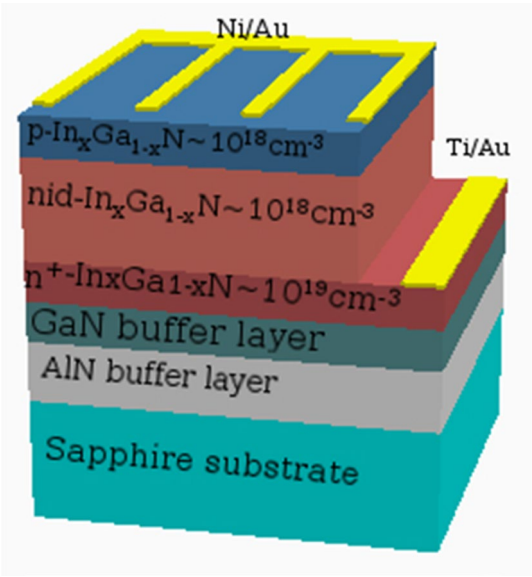

Fig. 1 Proposed $In_xGa_{1-x}N$ homo-junction solar cell structure for modeling

background assuming the p-type layers with a free hole concentration of 10^{18} cm^{-3}. Therefore, the doping concentrations in each layer will be the same with an electron and a hole concentration of 10^{18} cm^{-3}, respectively. The model includes the voltage dependence of the depletion region (W) and the effect of this on both the illuminated and dark current components. In very thin solar cells, such as the ones to be simulated here, these effects are very important and should be considered using a complete analytical model previously developed by our group [18], as explained below.

First, the bandgap Eg as a function of In content in $In_xGa_{1-x}N$ is calculated using a bowing parameter previously established in [13]:

$$E_g = E_g^{InN} + (1-x)E_g^{GaN} - bx(1-x) \quad (1)$$

where the energy band gaps of InN (E_g^{InN}) and GaN (E_g^{GaN}) are 0.7 eV and 3.42 eV, respectively. **x** is the Indium content and **b** is the bowing parameter (b = 1.43) [1, 5, 19].

The electron affinity (χ) is expressed in Eq. (2) [19, 20].

$$\chi_{In_xGa_{1-x}N} = \chi_{GaN} + 0.7\left(E_g^{GaN} - E_g\right) \quad (2)$$

where $\chi_{GaN} = 4.1$ eV.

The relative permittivity of the ternary alloy $\varepsilon_{In_xGa_{1-x}N}$ is expressed in Eq. (3) [20].

$$\varepsilon_{In_xGa_{1-x}N} = x\varepsilon_{InN} + (1-x)\varepsilon_{GaN} \quad (3)$$

where (ε_{InN}) and (ε_{GaN}) are 15.3 and 8.9, respectively.

The effective densities of states in the conduction and valence bands are expressed in Eqs. (4) and (5), respectively [19, 21].

$$N_C = (0.9x + 2.3(1-x))10^{18} \quad (4)$$

$$N_V = (5.3x + 1.8(1-x))10^{19} \quad (5)$$

The $In_xGa_{1-x}N$ intrinsic carrier concentration is expressed by Eq. (6).

$$n_i = \sqrt{N_V N_C}\exp\left(-\frac{E_g}{2kT}\right) \quad (6)$$

where k is the Boltzmann constant and T is the absolute temperature. N_c and N_v are the effective density of states in the conduction band and the valence band, respectively.

The electron and hole mobility are expressed as a function of doping concentration in Eq. (7) [19].

$$\mu_i(N) = \mu_{\min,i} + \frac{\mu_{\max,i} + \mu_{\min,i}}{1 + \left(\frac{N}{N_{g,i}}\right)^{\gamma_i}} \quad (7)$$

where i = n for electrons, i = p for holes, and N is the doping concentration, while the parameters $\mu_{max,i}$, $\mu_{min,i}$, $N_{g,i}$ and γ_i depends on the type of semiconductor material and their values, as listed in Table 1 [21]. Furthermore, the well-known diffusion coefficients and diffusion lengths are expressed as follows.

Table 1 Parameters used for the cell simulation

Parameters	Values
Absorption coefficient for a direct band gap semiconductor	$2.2\times10^5\sqrt{\frac{1240}{\lambda(nm)} - Eg}$
Bowing factor	1.43
Nd (cm^{-3})	10^{18}
Na (cm^{-3})	10^{18}
μ_e ($cm^2 V^{-1} s^{-1}$)	212.5
μ_h ($cm^2 V^{-1} s^{-1}$)	16.7
γ_i	1 for electrons and 2 for holes
μ_{max} (cm^2/V s)	1000 for electrons and 170 for holes
μ_{min} (cm^2/V s)	55 for electrons and 3 for holes
$N_{g,i}$ (cm^{-3})	2 for electrons and 3 for holes
GaN relative permittivity	8.9
InN relative permittivity	15.3
τ_p (s)	10^{-9}
τ_p (s)	10^{-9}
Base thickness d_n (nm)	200
Emitter thickness d_p (nm)	80
S_n (cm s^{-1})	1000
S_p (cm s^{-1})	1000

$$D_n = \frac{kT}{q}\mu_e, \quad D_p = \frac{kT}{q}\mu_h, \quad L_n = \sqrt{D_n\tau_n}, \quad L_p = \sqrt{D_p\tau_p}$$

An important parameter which determines the electric and photoelectric properties in a solar cell is the thickness of the space charge region (depletion region) in both the p-type and n-type sides of the junction. The depletion region depends on the doping concentration where high residual electron concentration causes a difficult p-type doping (as mentioned above). The depletion regions for a homo-junction are expressed by Eqs. 8–10 [18, 22].

$$Q_n = \left(\frac{\alpha L_n}{\alpha^2 L_n^2 - 1}\right)\left(\frac{\left(\frac{S_n\tau_n}{L_n} + \alpha L_n\right) - e^{-\alpha x_j}\left(\left(\frac{S_n\tau_n}{L_n}\right)\cosh\left(\frac{x_j}{L_n}\right) + \sinh\left(\frac{x_j}{L_n}\right)\right)}{\left(\frac{S_n\tau_n}{L_n}\right)\sinh\left(\frac{x_j}{L_n}\right) + \cosh\left(\frac{x_j}{L_n}\right)} - \alpha L_n e^{-\alpha x_j}\right) \tag{13}$$

$$Q_p = \left(\frac{\alpha L_p}{\alpha^2 L_p^2 - 1}\right)\left(e^{-\alpha(x_j+W)}\right)\left(\alpha L_p - \frac{\left(\frac{S_p\tau_p}{L_p}\right)\left(\cosh\left(\frac{H}{L_p}\right) - e^{-\alpha H}\right) + \sinh\left(\frac{H}{L_p}\right) + \alpha L_p e^{-\alpha H}}{\left(\frac{S_p\tau_p}{L_p}\right)\sinh\left(\frac{H}{L_p}\right) + \cosh\left(\frac{H}{L_p}\right)}\right) \tag{14}$$

$$x_n = \sqrt{\frac{2\varepsilon_0\varepsilon_{InGaN}N_a\left(v_{bi} - V\right)}{qNd\left[N_a + N_d\right]}} \tag{8}$$

$$x_p = \sqrt{\frac{2\varepsilon_0\varepsilon_{InGaN}N_d\left(v_{bi} - V\right)}{qNa\left[N_a + N_d\right]}} \tag{9}$$

$$W = x_n + x_p \tag{10}$$

where ε_0 is the permittivity in vacuum, q is the magnitude of the electron charge, v_{bi} is the built-in potential, V is the voltage across the diode, N_a and N_d are the acceptor and donor concentrations, respectively. The well-known built-in potential is reported elsewhere [18, 22]. In addition, it is worth mentioning that due to strong absorption coefficient a thin solar cell can be made, and thus, the effect of the voltage in the depletion region thickness should be included. This is because it impacts both the photo-collection within the depletion region and the reverse saturation current due recombination as shown below [18].

The following equations, from 11 to 15, were taken from references [18, 23]. The photocurrent density J_L is expressed by the following equation.

$$J_L = q\int Q(\lambda)F(\lambda)(1 - R(\lambda))d\lambda \tag{11}$$

where F(λ) is the density of the incident solar photon flux per unit bandwidth, R(λ) is the device reflectance and Q(λ) is the internal quantum efficiency:

$$Q(\lambda) = Q_n(\lambda) + Q_p(\lambda) + Q_{dr}(\lambda) \tag{12}$$

$Q_n(\lambda)$ is the contribution of electrons from the p-side, $Q_p(\lambda)$ is the contribution due to holes from the n-side, and Qdr(λ) is the contribution from the depletion region.

$$Q_{dr} = e^{-\alpha x_j}(1 - e^{-\alpha W}) \tag{15}$$

where $x_j = d_p - x_p$, $H = d_n - x_n$ and the emitter and absorber layer thickness are d_p and d_n, respectively.

The total current density is the difference of the photocurrent density and the dark current density (see Eq. 16). The dark current density is due to the diffusion current in the quasi-neutral regions, in addition to the generation-recombination current at the space-charge region. The well-known saturation current due to diffusion (J_0) is given in Ref. [18], and mainly depends on Eg and the diffusion lengths for the n and p type materials. The reverse saturation current due to recombination in the space-charge region is expressed by Eq. (17) below [18, 22, 23], where it is worth noting that if the carrier lifetime decreases, then the saturation current will increase. Previous experimental results [7, 12, 24] (PL, TEM and XRD) have shown that as the In-content increases, the optical and structural properties degrade. Therefore, as the In-content increases, the carrier lifetime should drop. However, in the absence of an expression relating the In content and the carrier lifetime, the carrier lifetime has been considered as constant. Of course, in this case, the reverse saturation current is underestimated for high In concentrations. The parameters used for the simulation are summarized in Table 1.

$$J_T(V) = J_L - J_0\left(e^{\frac{qV}{kT}} - 1\right) - J_{\text{Rec}}\left(e^{\frac{qV}{2kT}} - 1\right) \quad (16)$$

$$J_{Rec} = \frac{qn_i W(V)}{\tau_p} \quad (17)$$

J_L is the illumination current density defined above, J_0 is the dark diffusion current density [18], J_{Rec} is the dark space-charge recombination current density, n_i is the intrinsic carrier concentration and W, which depends on the applied voltage, has been defined before (see Eq. 10). As explained before, J_L and both dark current densities depend upon the voltage, and this is an important effect to be considered for very thin cells as is in this case. Usually this effect is not considered for conventional thick solar cells.

4 Results and discussions

In Fig. 2, the calculated output characteristics as a function of the In content for the $In_xGa_{1-x}N$ solar cells are shown. As expected, if the Indium content increases, the short circuit current (J_{sc}) increases due to the reduction of Eg. Nevertheless, the open circuit voltage (V_{oc}) and Fill factor (FF) decrease due to the increase in the reverse saturation current. In accordance to the Shockley–Queisser theory, the optimum Eg is at ~ 1.45 eV which implies that ~ 60% of In should be introduced into $In_xGa_{1-x}N$. However, solar cells with In concentrations greater than 40% have not been reported yet. $In_xGa_{1-x}N$ solar cells made with 40% of In have been claimed, but its experimental Eg resulted to be ~ 2.3 eV which is a high band gap for solar cell applications [14]. Figure 2 also shows the efficiency as a function of the In concentration. In concentration of 60% corresponds to Eg of 1.43 eV. Then, according to our calculations, the maximum $In_{0.6}Ga_{0.4}N$ solar cell efficiency is 18.9% which is less than 20.28% predicted for 65% In content in Ref. [20]. The explanation for this difference is due to two reasons, the first one and the most important is because Ref. [20] did not consider the dark current due to recombination at the space-charge region, which becomes a very important component for thin film solar cells. As a result, the estimated efficiency in [20] is not realistic. The second reason for the difference is that the assumed bandgap Eg in [20] is 1.31 eV, but the optimum bandgap should be 1.4–1.5 eV, as confirmed by the above results.

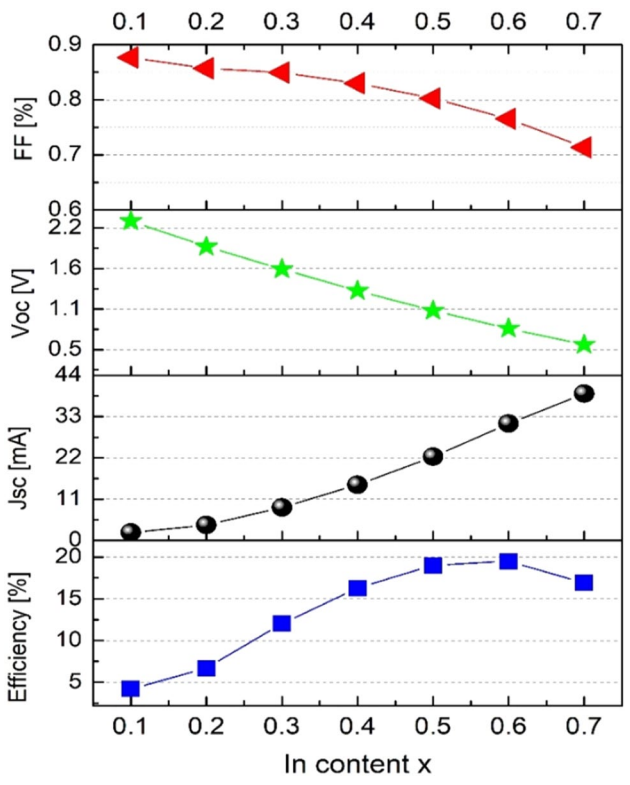

Fig. 2 **a** Fill factor (FF), **b** open circuit voltage (V_{oc}), **c** short-circuit current density (J_{sc}) and **d** efficiency, as a function of In content in the $In_xGa_{1-x}N$ homojunction solar cell

So, according to the state of the art, $In_xGa_{1-x}N$ solar cells with a In content higher than 40% have not been reported yet due to the technological challenges explained in this work. The main challenge is the control of the In incorporation avoiding the phase separation and the reduction of the carrier lifetime due to defects. According to our calculations, the maximum efficiency that can be obtained from an $In_xGa_{1-x}N$ homo-junction solar cell (when the reduction of carrier lifetime due the high In content is avoided) is ~ 18.9%. However, the available reports in the literature have shown diode ideality factors and shunt resistances in the range from 2.3 to 27.5 and 8×10^4 to 10^6 Ohm cm^2, respectively for $In_xGa_{1-x}N$ layers with an In content no more than 22% [15, 16, 25, 26]. These high ideality factors give evidence of strong recombination at defect traps in $In_xGa_{1-x}N$ solar cells. Thus, it is reasonable to expect that the lifetime will be reduced when the Indium content increases. This is because the In incorporation causes stress into $In_xGa_{1-x}N$ until the phase separation occurs. This stress might be released in the form of crystal defects resulting in a reduction of the minority carrier lifetime. Therefore, our prediction of the maximum efficiency (18.9%) is an optimistic prediction because we cannot model the effect of reduction of the minority carrier lifetime as the Indium content increases. Thus, experimental measurements for variation of lifetime as a function of the In content are necessary. In order to study the effect of In incorporation in $In_xGa_{1-x}N$ on the minority carrier transport properties, Fig. 3 shows the output properties of $In_xGa_{1-x}N$ solar cells

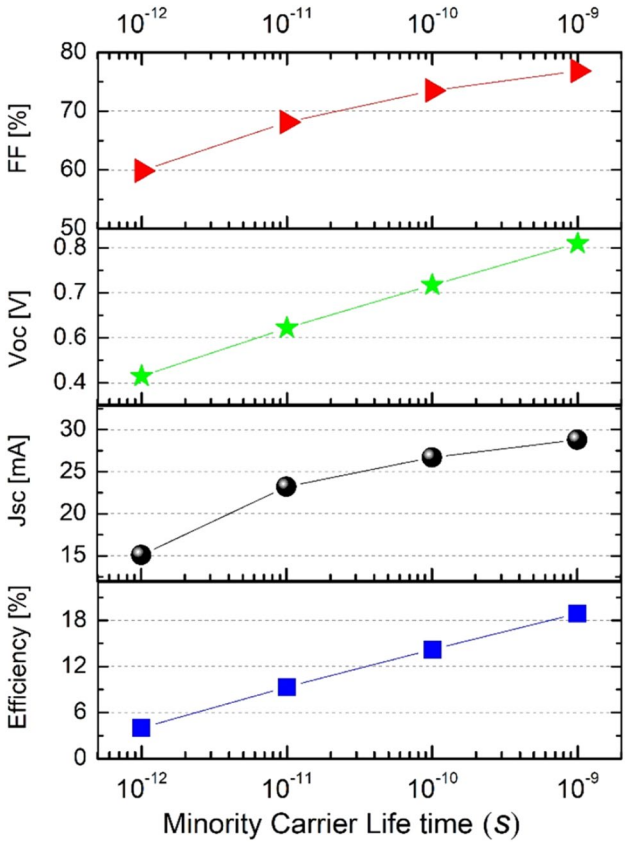

Fig. 3 $In_{0.6}Ga_{0.4}N$ homojunction solar cell output characteristics as a function of the carrier lifetime

with an In content of 60% as a function of the minority carrier lifetime. The most important result observed in Fig. 3 is that the efficiency can drop from 18.9 to 3.9% when the minority carrier lifetime is reduced from nanoseconds to picoseconds. Therefore, it is reasonable to claim that we are far from the dreamed high efficiency $In_xGa_{1-x}N$ solar cells and the technological issues mentioned above should be overcome, otherwise $In_xGa_{1-x}N$ solar cells will always be less efficient than the low-cost Silicon or thin-film solar cells technologies.

5 Conclusion

In this work, we have modeled $In_xGa_{1-x}N$ based homojunction solar cells considering realistic electrical transport parameters. In order to get better efficiency estimations, experiments for relating the carrier lifetime and the In content are required. However, the calculations revealed that the maximum efficiency will not be more than 19%. Therefore, due to its high cost and technological challenges, we consider that $In_xGa_{1-x}N$ might not become competitive with the most familiar and low-cost silicon cell technologies. In summary, we are far from the dreamed high efficiency $In_xGa_{1-x}N$ solar cells. Therefore, a new approach is needed, for example, using $In_xGa_{1-x}N$ nano-particles for making quantum dot solar cells or implementing a graded band-gap absorber layer (varying $\times$ gradually), as has been suggested for CdZnTe [17].

Funding Consejo Nacional de Ciencia y Tecnología de México (CONACyT) provided financial support to Mr. C. A. Hernández-Gutiérrez through a Ph. D. scholarship.

Compliance with ethical standards

Conflict of interest The authors declare that they have no conflicts of interest.

References

1. Bhuiyan AG, Sugita K, Hashimoto A, Yamamoto A (2012) InGaN solar cells: present state of the art and important challenges. IEEE J Photovolt 2(3):276–293
2. Pantha BN, Wang H, Khan N, Lin JY, Jiang HX (2011) Origin of background electron concentration in $In_xGa_{1-x}N$ alloys. Phys Rev B: Condens Matter 84:075327
3. Iliopoulos E, Georgakilas A, Dimakis E, Adikimenakis A, Tsagaraki K, Androulidaki M, Pelekanos NT (2006) InGaN (0001) alloys grown in the entire composition range by plasma assisted molecular beam epitaxy. Phys Status Solidi (A) 203(1):102–105
4. Kazazis SA, Papadomanolaki E, Androulidaki M, Kayambaki M, Iliopoulos E (2018) Optical properties of InGaN thin films in the entire composition range. J Appl Phys 123:125101
5. Wu J (2009) When group-III nitrides go infrared: new properties and perspectives. J Appl Phys 106:011101
6. Yamamoto A, Islam MR, Kang T-T, Hashimoto A (2010) Recent advances in InN-based solar cells: status and challenges in InGaN and InAlN solar cells. Phys Status Solidi C 7(5):1309–1316
7. Ponce FA, Srinivasan S, Bell A, Geng L, Liu R, Stevens M, Cai J, Omiya H, Marui H, Tanaka S (2003) Microstructure and electronic properties of InGaN alloys. Phys Status Solidi B 240(2):273–284
8. Fischer A, Kühne H, Richter H (1994) New approach in equilibrium theory for strained layer relaxation. Phys Rev Lett 73(20):2712
9. Fabien CAM, Gunning BP, Alan Doolittle W, Fischer AM, Wei YO, Xie H, Ponce FA (2015) ow-temperature growth of InGaN films over the entire composition range by MBE. J Cryst Growth 425:115–118
10. Ponce FA, Srinivasan S, Bell A, Geng L, Liu R, Stevens M, Cai J, Omiya H, Marui H, Tanaka S (2003) Microstructure and electronic properties of InGaN alloys. Phys Status Solidi B 240(2):273–284
11. Gherasoiu I, Man KY, Reichertz LA, Walukiewicz W (2014) InGaN doping for high carrier concentration in plasma-assisted molecular beam epitaxy. Phys Status Solidi C 11:381
12. Pantha BN, Sedhain A, Li J, Lin JY, Jiang HX (2009) Electrical and optical properties of p-type InGaN. Appl Phys Lett 95:261904
13. Greco G, Iucolano F, Roccaforte F (2016) Ohmic contacts to gallium nitride materials. Appl Surf Sci 383:324–345
14. Valdueza-Felip S, Ajay A, Redaelli L, Chauvat MP, Ruterana P, Cremel T, Jiménez-Rodríguez M, Kheng K, Monroy E (2017)

Pin InGaN homojunctions (10–40% In) synthesized by plasma-assisted molecular beam epitaxy with extended photoresponse to 600 nm. Sol Energy Mater Sol Cells 160:355–360
15. Fabien CAM, Maros A, Honsberg CB, Alan Doolittle W (2016) III-nitride double-heterojunction solar cells with high in-content InGaN absorbing layers: comparison of large-area and small-area devices. IEEE J Photovolt 6(2):460–464
16. Valdueza-Felip S, Mukhtarova A, Grenet L, Bougerol C, Durand C, Eymery J, Monroy E (2014) Improved conversion efficiency of as-grown InGaN/GaN quantum-well solar cells for hybrid integration. Appl Phys Express 7:032301(1)–032301(4)
17. Morales-Acevedo A (2011) Analytical model for the photocurrent of solar cells based on graded band-gap CdZnTe thin films. Sol Energy Mater Sol Cells 95:2837–2841
18. Acevedo-Luna A, Bernal-Correa R, Montes-Monsalve J, Morales-Acevedo A (2017) Design of thin film solar cells based on a unified simple analytical model. J Appl Res Technol 15:599–608
19. Benaicha M, Dehimi L, Sengouga N (2017) Simulation of double junction $In_{0.46}Ga_{0.54}N$/Si tandem solar cell. J Semicond 38(4):044002
20. Zhang X (2007) Simulation of $In_{0.65}Ga_{0.35}N$ single-junction solar cell. J Phys D Appl Phys 40:7335–7338
21. Bouzid F, Hamlaoui L (2012) Investigation of InGaN/Si double junction tandem solar cells. J Fundam Appl Sci 4:59–71
22. Sze SM, Ng KK (2007) Physics of semiconductor devices, Chap 2. Wiley
23. Garozzo M, Parretta A, Maletta G (1986) GaAs shallow homojunction solar cells fabricated on thin epitaxial films by a simple Zn solid state diffusion method. Sol Energy Mater 14:29–49
24. Valdueza-Felip S, Bellet-Amalric E, Nuñerz-Cascajero A (2014) High In-content InGaN layers synthesized by plasma-assisted molecular-beam epitaxy: growth conditions, strain relaxation, and In incorporation kinetics. J Appl Phys 116:233504
25. Arif M (2017) Improving InGaN heterojunction solar cells efficiency using a semibulk absorber. Sol Energy Mater Sol Cells 159:405–411
26. Liou BW (2011) Design and fabrication of $In_xGa_{1-x}N$/GaN solar cells with a multiple-quantum-well structure on SiCN/Si (111) substrates. Thin Solid Films 520:1084–1090